Speckle Interferometry with the OCA Kuhn 22" Telescope

Rick Wasson
Murrieta, California
ricksshobs@verizon.net

Abstract: Speckle interferometry measurements of double stars were made in 2015 and 2016, using the Kuhn 22-inch classical Cassegrain telescope of the Orange County Astronomers, a Point Grey Blackfly CMOS camera, and three interference filters. 272 observations are reported for 177 systems, with separations ranging from 0.29" to 2.9". Data reduction was by means of the REDUC and Speckle Tool Box programs. Equipment, observing procedures, calibration, data reduction, and analysis are described, and unusual results for 11 stars are discussed in detail.

Introduction

Membership in the Orange County Astronomers (OCA), one of the largest and most active amateur astronomy clubs in the United States, has many privileges, not the least of which is access to the fine Kuhn 22-inch (0.56 meter) Cassegrain telescope, located at the club's Anza observing site, with fairly dark skies at 4300 feet elevation, in the hills about 15 miles northeast of Mount Palomar Observatory. OCA member William Kuhn led a volunteer effort of many OCA members in designing and building the telescope, named after him. The observatory became operational in 1984, and has been used occasionally for research, particularly discovery of supernovae and asteroids. It is open to all club members and guests every month at new-moon star parties, for viewing all types of celestial wonders.

The combination of my long-time OCA membership, experience in observing double stars (Wasson, 2014), and the convenient Anza site located only 37 miles from my home, seemed a natural fit to attempt a new type of research - Speckle Interferometry - which would benefit greatly from a larger aperture than my own 12-inch telescope.

I was encouraged by a workshop on Speckle Interferometry presented by Russ Genet and Dave Rowe at the Society for Astronomical Sciences (SAS) meeting in June 2015.

From its inception in the 1970s until recently, Speckle Interferometry was practiced only by professional astronomers and graduate students, using specialized equipment at major observatories. The example shown in Figure 1 demonstrates the potential of Speckle Interferometry to improve measurement accuracy for close binaries, reducing uncertainty and eventually producing a high-quality orbit solution.

The technological revolution in small, sensitive, fast, moderately-priced CMOS cameras, now used extensively by amateurs to make exquisite planetary images, has also opened the Speckle imaging field to amateurs. The last piece of the puzzle, easy-to-use software for processing Speckle images, has only become available since 2010, making amateur Speckle Interferometry practical for the first time.

Why Observe Double Stars?

Everything we know about stars is based on observing their light with a range of instruments, to measure or derive their basic properties. The most fundamental property of any star is its mass, which determines how rapidly nuclear fusion proceeds in its core, and thus its intrinsic brightness and its life expectancy.

The only direct way to determine the mass of stars is by observing them in binary systems. Orbital velocity (measured by Doppler shift) and period are driven by the stars' masses and distance apart. We need to know the apparent size of the orbit and its distance from us, to find the true physical size of the binary star orbit. Distance is measured most accurately by parallax; the Hip-

(Text continues on page 224)

Speckle Interferometry with the OCA Kuhn 22" Telescope

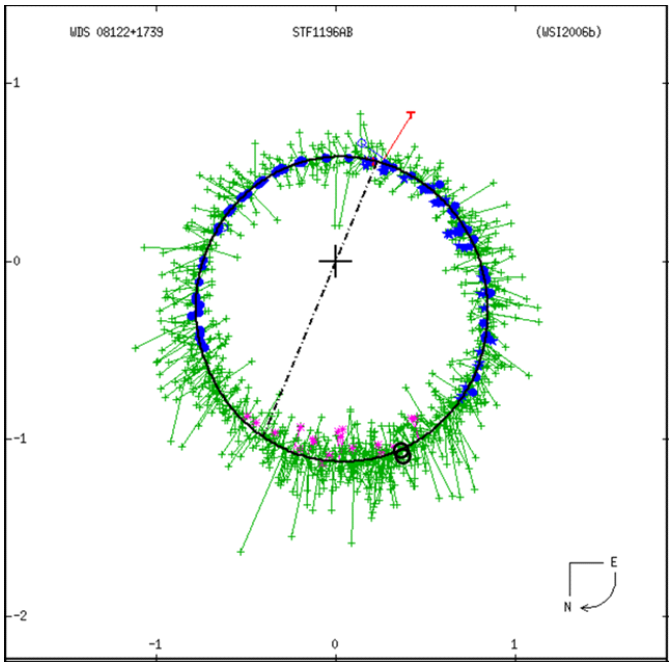

Figure 1. The orbit of STF1196AB, the brightest two components of the well-observed, multiple star system Zeta Cancri ("Tegmen"). These two stars (A and B) orbit each other in 59.6 years. The large + symbol represents the primary star. Solid blue dots (speckle interferometry) and small + symbols (visual micrometer) are measurements of the secondary star position. Note the improved precision (reduced scatter) of the speckle points as compared to visual observations. The ellipse is the best current orbit solution, giving extra weight to the speckle data. Lines from data points to the ellipse indicate the time on the orbit at which the data point was taken. The scales are in arc seconds. Two new speckle points from this paper are shown as black circles, added to the plot by the method of Buchheim, 2017.

parcos satellite of the 1990s made great improvements in distance accuracy, and the next-generation Gaia satellite is now in operation. That leaves the apparent orbit ellipse as the last measurement needed to define the stellar masses accurately.

Surprisingly, less than 60 binary star systems have *accurately* measured (definitive) orbits, so the quality of our models of stellar evolution hangs on this remarkably small sample! Many systems with large orbits are so slow that they have not completed a single orbit since measurements began (about 250 years ago by William Herschel), and many "fast" orbits appear so close together that they can only be resolved by very large telescopes. But many others, some having orbital periods of a few decades, are near enough that their separation can theoretically be resolved and measured by the Kuhn 22-inch aperture, for which the "Rayleigh limit" resolution is about 0.3 arc-sec; thus, the Kuhn 22 -inch telescope has the potential to help refine the accuracy of stellar masses – among the most fundamental properties in astronomy!

The "Seeing" Problem

The theoretical angular resolution of any telescope depends only on the wavelength of light and the telescope aperture - the larger the aperture, the smaller and closer are details which can be resolved. But for telescopes larger than about 4 inches, atmospheric "seeing" begins to limit the resolution that can be achieved. The problem, of course, is that the sharp, diffraction-limited image of a star is continuously chopped up, shifted and smeared in random ways by small atmospheric cells of variable temperature, density and refraction index, creating an image that is blurred into the "seeing disk."

A most remarkable fact was discovered and demonstrated by Anton Labeyrie in 1970: the full-resolution information of a double star image still exists in the scrambled "seeing" disk! If very short exposures are taken to "freeze" the motion, each frame shows a pattern of small "speckles." This is the interference pattern of images formed by many, small, separate atmospheric cells, superimposed upon each other, swirling within the seeing disk. Constructive interference forms a bright speckle. Picture the moving pattern of light "speckles" on the bottom of a swimming pool, created by the wavy surface acting like a bunch of small, moving, tilting lenses.

The power of Speckle Interferometry is to recover almost all the information contained in a diffraction-limited image of a double star formed by the full telescope aperture. Fourier Transform analysis finds dimensional frequency information (spacing and orientation) from the speckle patterns of each frozen image; the information gathered from many images is then averaged. Those speckles related to the diffraction-limited image add together, while randomly positioned speckles do not. Quality is enhanced by observing a single reference star, nearby on the sky and near in time; deconvolution with the reference star helps cancel distortions which are common to both the single and double star images.

Equipment - Telescope

The Kuhn 22-inch telescope is an f/8 classical Cassegrain design on an equatorial fork mount. It has encoders on both axes, and "Go-To" capability using an older version of TheSky software (www.bisque.com). Although it was built decades ago, club members have upgraded and maintained it well. It can find most objects within a few arc minutes, well within a medium power eyepiece field. Tracking errors from frame to frame are usually smaller than the seeing movements caused by the atmosphere, which are stopped anyway by taking short exposures (typically 10 to 40 millisec-

onds), so the telescope is suitable for high magnification Speckle Interferometry.

Equipment - Camera

For all the observations in this paper, I used a Point Grey BlackFly 23S6M-C high-speed monochrome camera, having a Sony IMX249 CMOS detector with 5.86μ square pixels in a 1920x1200 array, and a global shutter (https://www.ptgrey.com). This camera was chosen because of its fairly large detector (11.2mm x 7.0mm), advertised low read noise (7e- rms), high Quantum Efficiency (82% peak at 500nm), high speed USB3.0 interface (more than 30 fps full frame), and moderate price ($495). A larger-than-usual CMOS detector was considered important for the following reasons:

1. Prior experience with my 12-inch Go-To Dobsonian telescope at home had shown that it may be difficult to acquire and track faint stars at high magnification required for speckle work, and the pointing and tracking performance of the 22" was unknown to me at the time.

2. I planned to investigate the sidereal drift method to calibrate images for orientation and plate scale (discussed in detail below), where a larger field, giving a longer drift, is helpful.

Equipment – Eyepiece Projection

High magnification is required in Speckle Interferometry, so that details of the distorted star images can be seen; individual speckles, which are comparable in size to the Airy disk, should each cover at least several pixels. Proper magnification is a balance between magnifying enough for adequate pixel sampling of the image, but not magnifying so much that S/N is low and fainter stars cannot be detected. I have had success with plate scales of about 0.07 arc-sec/pixel, so that the Airy Disk spans about 8 pixels, a value recommended by Dave Rowe (Rowe, 2016) based on simulation studies. For the Kuhn aperture and detector pixel size, this corresponds to about f/30. A spreadsheet was developed to estimate the magnification achieved for eyepiece projection or a Barlow lens.

For all the observations presented here, magnification was accomplished by eyepiece projection, using a Baader Hyperion 10mm eyepiece, T2 threaded adapters on the eyepiece and camera, and T2 projection tubes. Screw threads helped make a solid, rigid optical assembly. A flip mirror and 23mm illuminated reticle eyepiece were used to find, identify and center target stars. The cabling is clean and simple: a single 3-meter USB3.0 cable supplied 5VDC power to the camera and carried data to the laptop computer. My setup ready for speckle interferometry is shown in Figure 2.

Equipment - Filters

In early observations, a red filter was used to minimize color dispersion of the speckles. It was simply screwed into the $1^{1}/_{4}$-inch threads on the front of the Baader Hyperion eyepiece. After purchasing a ZWO manual filter wheel (https://www.zwo.com), additional filters were also used during each observing run.

Table 1 gives the filter characteristics. The filters are not members of any photometric standard series,

Figure 2. Left: Speckle Interferometry installation on the Kuhn 22" Telescope. A single blue USB3.0 cable connects the camera to the laptop on the white table at lower right. Right: Close-up of the simple finding and magnification optics: an illuminated reticle eyepiece is at top in the flip mirror; below are the Baader Hyperion 10mm eyepiece, projection tubes, and tiny (30mm cube) camera, attached to the blue USB3.0 cable. No filter wheel was used in this early configuration.

such as Johnson-Cousins or Sloan. However, these interference filters are similar in bandpass to some of the photometric standard filters, with significant advantages over colored glass: sharper cutoff, symmetric transmission profile, much better durability and lower price. If differential photometry of close binary stars becomes practical in the future, it is believed that the G and R filters, which are part of the Baader LRGB series for CCD imaging, will transform well to the standard photometric systems, because G has 50% transmission wavelengths very close to Johnson V, and R has the same 50% transmission width as Cousins R, but shifted about 15 nm farther red. The "IR742" filter is not a good match to any photometric filters, but was used in attempting to observe faint late-type stars. Unfortunately, the QE of the IMX249 CMOS detector is low in the near IR, only about 16% at 823nm. However, some recent Sony CMOS detectors have improved QE, even approaching that of back-illuminated CCDs.

Preparing for a Speckle Run

Double star targets were chosen by searching the Washington Double Star (WDS) Catalog, using the online tool developed by Tom Bryant (2015), by way of his web site. The search parameters generally employed were:

- 3.0" > Separation < 0.3" (0.3" is the approximate Rayleigh criterion for 22" aperture)
- Primary star brighter than magnitude 10
- Magnitude difference less than 3
- Declination between +70° and -30°
- Each search limited to a 2-hour RA window.

Within any given RA range, the WDS provides many candidates. Those with at least a preliminary orbit were preferentially selected, with the goal of adding quality speckle points to help refine the orbits. Other target stars included some late spectral types (K0 and later) and Hipparcos discoveries that have shown some movement. For each selected double star, the WDS data line was copied into an EXCEL spreadsheet. Multiple sheets, each containing targets in a 2-hour RA window, constituted a Master Target List workbook. Some spreadsheets were printed, to act as both the target list and log for hand-written notes at the telescope.

For some stars, more information was found at the Italian website Stelle-Doppie (Sordiglioni, 2016), including SAO number, orbital period, and current orbit ephemerides for separation and PA. The WDS orbit plots were also copied and hyper-linked into the spreadsheet for quick reference. For observations made after June 2016, the "master" spreadsheet was copied, then used as a computer log during the run, by editing recorded sequence numbers and notes into the spreadsheet in real time, eliminating the paper log.

I have found that the easiest way to identify target stars at the telescope is by SAO catalog number, so the SAO number of each target double star, and a nearby single "reference" star (used for deconvolution during data reduction) were added to the Master Target List spreadsheets. This was a time-consuming process, but saved observing time. Dave Rowe has recently developed a WDS search program WDS1.0 (Rowe, 2017) which searches the WDS catalog for double stars according to user-input parameters, but also has the very useful feature of listing all nearby SAO stars by magnitude, spectral type and distance from the double, thus saving a great deal of manual search time. The general faint limit of about 10th magnitude for SAO stars seems well suited to the 22" for my camera, magnification and typical 30-millisecond exposures; fainter stars are often buried in the noise, but there are plenty of suitably bright targets.

At the Telescope

Observing runs were made only about once per month, for convenience in scheduling, allowing choice of "good" nights, and giving plenty of time for data reduction. After following the checklist for opening the OCA observatory and preparing the Kuhn telescope and control computers, the Speckle Interferometry optical train is screwed together and installed in the Cassegrain 2-inch focuser. The cable from the camera is plugged into a USB3.0 port on the laptop, and the data acquisi-

Table 1. Filter characteristics. These interference filters typically have a sharp rise and fall of about 10 nm width, and a high, nearly constant transmission plateau (95+%). The "IR742" filter is a long-pass IR transmission filter; the asterisks indicate convolved characteristics: the filter transmission times the QE of the Sony IMX249 monochrome CMOS detector, as measured by Point Grey (https://www.ptgrey.com).

Filter	Manufacturer Name	50% Band Pass (nm)	Center Wavelength (nm)	Width (nm)	Peak Transition
G	Baader G (CCD)	495 - 575	534	80	96%
R	Baader R (CCD)	585 - 690	636	105	98%
IR742	Astronomik ProPlanet 742	740 – 1000 *	823 *	250 *	30% *

tion software FireCapture (Edelmann, 2015) is started. This program, designed primarily for planetary imaging, is used because it can handle many types of cameras and can output frames as FITS files, which is a convenient format for Speckle data reduction.

The telescope is slewed to a bright star, the star is centered in the illuminated reticle eyepiece, then focused and centered in the camera display screen, and "synced," to be sure TheSky software knows accurately where the telescope is pointing. The highly-magnified, turbulent image of the moderately bright star is focused until speckles become clearly visible on the laptop screen. Since the telescope truss tube is made of welded steel tubing, and the mirror is about 3 inches thick, focus can change slightly as the telescope cools through the evening. Re-focusing is needed when the speckles gradually become "soft" or smeared, or the star image shape appears distorted in a systematic way. Re-focus movements were very small, and the possible effect on image scale calibration was not investigated.

After selecting a target double star, typing in its SAO number, and clicking the "slew" command, the telescope comes to life, majestically but quietly "humming" its way toward the target, which is almost always seen in the eyepiece of the flip mirror. After centering in the illuminated reticle eyepiece, the star is always close to the center of the camera CMOS chip displayed on the laptop. The double star target is centered and a small "Region of Interest" (ROI) selected in FireCapture, usually a 512x512 pixel patch (about 40x40 arc-sec) near the center of the chip. With the filter, exposure and camera settings confirmed, FireCapture is ordered to record 1000 frames, and I watch as the star boils and dances for about 30 seconds, to be sure it doesn't drift too near an edge of the ROI field. Only bright and well-separated double stars (more than about 1 arc-sec) are obviously seen as double on the screen; a tight and/or faint companion is invisible in the seeing mess, but it is still there! 1000 frames are taken as a good sample of the random variations in speckle patterns produced by the atmosphere, to get an accurate average of the speckle spacing and orientation information.

The next target is a "reference" star, which is a nearby *single* star, used later for deconvolution in data reduction. All the same optical imperfections that affect the double star are captured in the reference star as well, including even focus and some atmospheric effects. By Fourier Transform "deconvolution," these small effects are cancelled from the double star data, greatly improving and sharpening the Autocorrelation end product.

Although only one sequence is required for a speckle measurement, several sequences may be taken, to provide improved S/N or statistical samples for defining uncertainty of the final measurement. More frames are generally better, especially for fainter, closer doubles.

Light passing through the atmosphere is affected by atmospheric dispersion: the atmosphere refracts different wavelengths by different amounts, forming a miniature spectrum at focus. This effect may be noticeable at very high magnification, and increases rapidly at large zenith angles. An atmospheric dispersion corrector (ADC) was not used for these observations, but "smearing" was minimized by using filters to restrict the wavelength range, and by usually limiting observations to stars within about 40 degrees of the zenith. Nevertheless, in some results, the "smearing" was noticeable, reducing the measurement accuracy somewhat.

Calibration

The Drift Calibration method was used to calibrate each night's data for Plate Scale and Camera Orientation on the sky. Multiple drifts were made throughout the night, usually on brighter reference stars, and the average results of all drifts were used to reduce all the speckle data for that night. This method applies only to equatorially-mounted telescopes, and no adjustments can be made which could change the magnification or rotate the camera.

To make a Calibration Drift sequence, a special ROI was used, having full E-W frame width (about 2½ arc-minutes) but only 300 pixels in N-S height; this ROI speeds up the frame rate and reduces hard drive storage space. A moderately bright star was moved to the east edge of the field, then the recording sequence was started and immediately the circuit breaker powering the telescope RA drive motor was turned off. After the star drifted at the sidereal rate from the eastern to the western edge of the field, the breaker was turned back on. The telescope was driven west with the hand paddle control until the star was again recovered. A drift typically takes about 10 seconds near the equator, and longer at higher declination. A series of several drifts was usually made with the same star. After the drift series was completed, TheSky was "synced" once more to re-establish accurate telescope pointing.

The sidereal drift path of the star describes the true east-west direction, distorted somewhat by the star bouncing around in the seeing disk, or possibly by a breeze moving the telescope, so the more drifts the better. The FireCapture acquisition software writes the computer clock time (to the nearest millisecond) to the FITS header of each frame. The exposures are short enough to stop the sidereal motion in each frame, as

well as the seeing motion. Thus, the drift sequence records hundreds of star positions (seeing-distorted image centroid, in pixels) at known times. The least-squares slope of the star positions calibrates the rotation angle of the camera relative to the true east-west direction on the sky. Changes in star position versus time, and the known sidereal rate (a function only of star declination) are used to calculate the pixel scale calibration constant (arc-sec / pixel).

This drift analysis was originally done - very laboriously - in a spreadsheet, but is now part of the Speckle Tool Box (STB) data reduction program (Harshaw, Rowe, and Genet, 2017), making it *very much* easier, faster, and more accurate. Figure 3 is an example of one night's calibration data. Each drift sequence was first edited in REDUC (Losse, 2015) to delete frames having the star not in the field, or overlapping the edge. REDUC then calculated the camera rotation angle on the sky by least-squares fitting the star position from all valid frames. The same set of valid frames was then processed in STB, calculating both the drift angle and pixel scale factor, using the computer clock time written to the FITS header. For each drift, the camera angle results from REDUC and STB usually agree very closely: within a few hundredths of a degree.

Very rarely, a laptop clock "glitch" was found to occur. The cause may be either intensive processing by a program other than the FireCapture image acquisition program, or by an automatic clock update during sequence acquisition. The quad processors of the Intel i7-based laptop make such events very rare, but when they occur they are easily identified: there is a large effect on pixel scale, which depends on self-consistent time within the sequence, but no effect on the drift angle, which does not depend on time.

Data Reduction and Speckle Analysis

Speckle Interferometry data reduction is accomplished by Fourier Transform mathematical analysis of dimensional frequency information - that is, the spacing and orientation of the speckle patterns in every frame. It requires some intense "number crunching!" Processing includes taking Fast Fourier Transforms (FFT) of all 1000 individual frames in the binary star sequence, then averaging the results. The same operations are done for the sequence of single "reference" star frames. In "deconvolution," the average transform of the double is divided by that of the reference, tending to cancel aberrations and distortions that are common to both sets. The cancelling benefit can include optical aberrations (central obstruction, mirror imperfections, coma, focus errors, etc.), and even some atmospheric effects!

In the last step of processing, an inverse Fourier Transform is taken to give an "Auto-correlogram." Although it may look like a picture of the stars, it is no longer a real image. But the auto-correlogram still contains the near-diffraction-limited information from which measurements are made. An example is shown in Figure 4.

Fortunately, the "heavy lifting" of Fourier Transform math for speckle image processing has been implemented already, and is transparent to the user. At least two freeware programs for Speckle data reduction are available on-line to amateur astronomers, by request of the authors: REDUC (Losse, 2015) and Speckle Tool Box (STB) (Harshaw, Rowe, and Genet, 2017). STB1.05 was used for all position angle (PA) and separation measurements presented here.

STB marks the secondary peak chosen to measure PA and separation, with a purple "ship's wheel" symbol, as seen in Figure 4. Measurements are based on

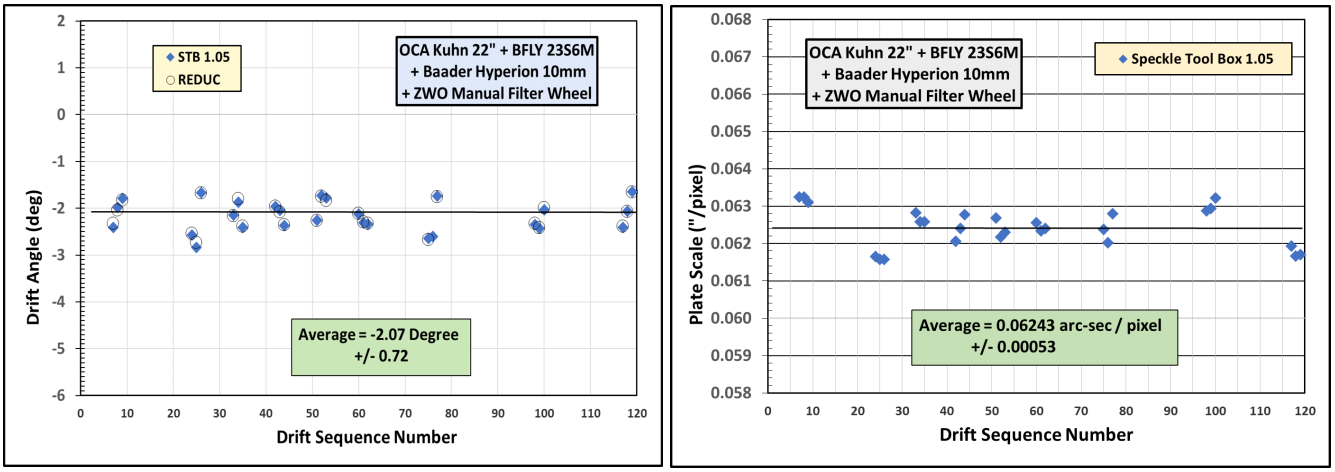

Figure 3. Results of Drift Calibration sequences during a Speckle run in November 2016, using the STB and REDUC programs. Left: Drift Angle. Right: Plate Scale.

calculation of the centroid of the secondary peak, to a small fraction of a pixel. Because the speckle images, and resulting auto-correlogram peaks, are over-sampled (typically ~8 pixels across the Airy disk), the centroid location is very accurate, yielding accurate measurements.

The STB default orientation is north down, east right like most reflecting telescopes show, and like the WDS orbit plots. However, I always orient my camera with north up and east left, as though looking at the sky with the pole up – it's just easier for my foggy brain to think about late at night - so my orientation is rotated 180 degrees. Therefore, I always choose the peak in the opposite quadrant, which gives the correct numerical PA value. The observer must be careful to select the peak consistent with actual image orientation. The same convention and care must also be used in interpreting the camera calibration angle from the STB Drift Calibration tool.

Speckle Measurement Uncertainty and Observation Quality

Quality of the speckle measurements was not rigorously evaluated. Usually only one sequence of 1000 frames was recorded, and no statistical information was calculated. For very faint systems, 2000 to 5000 frames were sometimes recorded, aiming to improve S/N - but even then, all the frames were processed as one sequence, yielding no statistics.

Standard deviation was calculated for calibration data, since many samples were acquired each night. Standard deviation of the camera drift angle for all nights ranged from 0.01 degree to 0.72 degree, with an average of 0.26 degree. Standard deviation of pixel scale ranged from 0.25% to 2.82%, with an average of 0.83%. Therefore, it is assumed that the *minimum* uncertainty of PA is roughly 0.3 degree, and the *minimum* uncertainty of separation is roughly 0.8%. The total uncertainty of the measurements, considering unknown error sources besides calibration, must be greater, perhaps more than twice these values. Therefore, the typical uncertainties of the measurements presented here are estimated to be roughly +/-1 degree for PA, and +/-0.01 arc-sec for separation.

A *qualitative* figure of merit was assigned to each measurement, as shown in Table 2, with values rated from 1 to 7. When measuring PA and separation in STB, the auto-correlograms of most doubles were bright and wide enough to yield very "solid," repeatable solutions. Observations with mild atmospheric dispersion, causing "smeared" auto-correlogram peaks, were assigned quality 2. For very close and/or faint doubles, the measurements were sometimes difficult. Values of 5 are not considered very accurate, because the secondary peak of the auto-correlogram was not clearly separated from the central peak, making its centroid location uncertain. Values of 6 are also unreliable because the faint secondary peak was distorted by, or not clearly distinguishable from, background noise. A value of 7 indicates that no reasonable measurement was possible. In Table 3, those measurements having poor quality of 5, 6 or 7 are flagged in color.

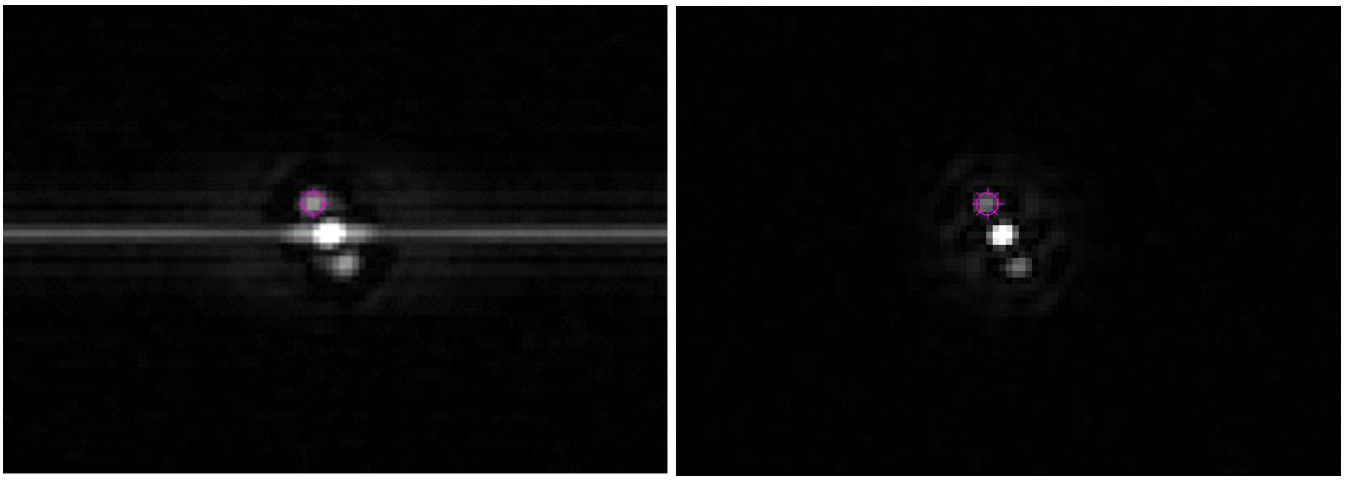

Figure 4. The Auto-correlogram of the binary star BU688AB, WDS magnitudes 8.1 and 8.6, observed with the Kuhn 22" and R filter on September 1, 2016. The bright central peak corresponds to the Airy disk of the primary star, always centered in the frame. The Fourier Transform process creates two equally valid peaks corresponding to the secondary star; they have the same separation, but are exactly 180 degrees apart. Selection of the correct one (purple "ship's wheel" symbol) is based on prior observation trends or an estimated orbit. Left: The horizontal line is an artifact of line pattern ("read") noise of the CMOS camera. Right: Employing the Interference and High Pass filtering features of STB cleans up the Auto-correlogram beautifully. The measured Separation was 0.406 arc-sec, PA=195.43 deg.

Table 2. Qualitative Figure of Merit for Speckle Measurements. A Figure of Merit code number is given for each measurement in Table 3.

Figure of Merit	Notes Related to Quality of the Observations
1	Bright, clear Auto-correlogram. Solid measurement.
2	Some distortion of fringes or peaks, but measurement solid.
3	Close, but measurement clear, solid.
4	Companion faint, but measurement clear, solid.
5	Very close. Measurement uncertain.
6	Companion very faint. Measurement uncertain.
7	Companion too close or faint. Measurement NOT valid.

Double Star Separation and Position Angle Measurements

Speckle measurements were made from September 2015 through December 2016, observing with the OCA Kuhn 22-inch telescope approximately one night per month. A total of 177 double stars were observed in up to three filters, with separations ranging from 0.29 to 2.9 arc-seconds, and secondary WDS magnitudes from 5.5 to 9.9. The speckle measurements are presented in Table 3.

Discussion of Selected Double Stars

Many of the stars observed in Table 3 are binaries with at least a preliminary orbit. Some were found to have large Separation or PA O-C values, relative to the orbit ephemerides. In addition, a few stars had large movement from relatively few prior measures. Some of those, with O-C greater than 0.1" separation or 10 degrees PA, are discussed below.

The binary **00022+2705 BU733AB** (85 Peg) has a very high proper motion (+830-989) and short period (26.28 years). It was observed in the R filter at a separation of 0.309", barely above the Rayleigh criterion of 0.286". The night was marginal, with occasional high clouds, and the speckle solution centroid was uncertain (figure of merit 6). The results are shown in Figure 5.

The Hipparcos-Tycho satellite observed **02194 +6616 TDS2201** as double (PA=123.5 deg, separation=0.32") in 1991, but this remains the only prior observation. The current measure of Table 3, in the "R" filter, is PA=94.93 deg, separation=0.462". However, this observation was rated only as quality 6 (Table 2), because the companion was very faint, the secondary peaks were barely above the background noise, as seen in Figure 6, and the secondary peak centroid was uncertain. There was also a second pair of peaks, shown in the speckle auto-correlogram of Figure 6. The peak at 94 degrees was chosen because it was slightly stronger, closer to the Tycho value, and the "smeared" shape of

(Continued on page 236)

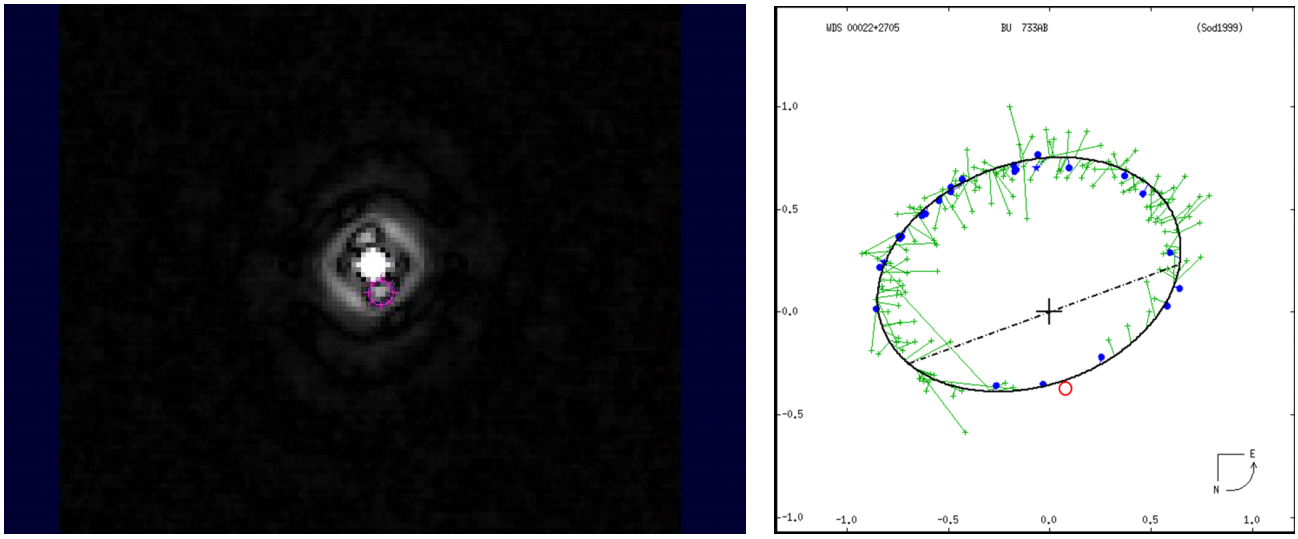

Figure 5. Left: BU733AB STB auto-correlogram. Right: Orbit plot from the WDS 6th Orbit Catalog, with the new speckle point

Speckle Interferometry with the OCA Kuhn 22" Telescope

Table 3. Speckle measurements in 2015 and 2016, using the OCA Kuhn 22-inch telescope, Point Grey BlackFly-U3-23S6M-C CMOS camera, and interference filters. The columns are: observation date, WDS designation, WDS discovery designation, filter (Table 1), position angle observed (degrees), separation observed (arc-seconds), and qualitative figure of merit (Table 2).

Obs Date	WDS	Discovery	Filter	ThetaO	RhoO	Quality
2015.846	00014+3937	HLD60	R	166.72	1.328	4
2015.934	00022+2705	BU733AB	R	12.10	0.385	6
2015.846	00028+0208	BU281AB	R	159.74	1.579	1
2015.958	00049+3005	A1250AB	R	41.22	0.885	1
2016.843	00063+5826	STF 3062	G	359.36	1.528	1
2016.843	00063+5826	STF 3062	IR742	359.41	1.503	1
2015.934	00063+5826	STF3062	R	358.08	1.548	1
2016.843	00063+5826	STF 3062	R	359.40	1.509	1
2015.958	00065+1250	TDS1293	R	4.91	0.430	3
2016.843	00118+2825	BU 255	G	66.24	0.447	4
2016.843	00118+2825	BU 255	IR742	71.86	0.467	4
2016.843	00118+2825	BU 255	R	67.53	0.432	1
2016.843	00121+5337	BU 1026AB	G	321.12	0.355	4
2016.843	00121+5337	BU 1026AB	IR742	329.64	0.371	3
2016.843	00121+5337	BU 1026AB	R	323.19	0.338	5
2016.994	00308+4732	BU394AB	G	277.87	0.809	1
2016.994	00308+4732	BU394AB	IR742	277.62	0.789	2
2016.994	00308+4732	BU394AB	R	278.13	0.811	1
2016.994	00550+2338	STF73AB	G	331.58	1.145	1
2016.994	00550+2338	STF73AB	IR742	331.37	1.132	1
2016.994	00550+2338	STF73AB	R	331.44	1.144	1
2015.934	01006+4719	MAD1	R			7
2015.958	01006+4719	MAD1	R	1.27	0.836	1
2015.958	01014+1155	BU867	R	352.46	0.659	1
2015.846	01030+4723	STT21	R	175.23	1.294	1
2015.958	01097+2348	BU303	R	293.52	0.607	1
2015.846	01106+5101	BU235AaAb	R	140.41	0.835	1
2016.843	01234+5809	STF 115AB	G	158.45	0.403	1
2016.843	01234+5809	STF 115AB	IR742	160.43	0.448	1
2016.843	01234+5809	STF 115AB	R	158.82	0.405	1
2016.994	02037+2556	STF208AB	G	344.32	1.419	1
2016.994	02037+2556	STF208AB	IR742	344.30	1.413	1
2016.994	02037+2556	STF208AB	R	344.24	1.410	1
2016.994	02140+4729	STF228	G	303.39	0.653	1
2016.994	02140+4729	STF228	IR742	304.92	0.647	1
2016.994	02140+4729	STF228	R	303.77	0.654	1
2015.934	02186+4017	EGG2Aa,Ab	R			7
2015.958	02194+6616	TDS2201	R	94.93	0.462	6
2015.958	02211+4246	STF248	R	206.69	0.722	2
2015.934	02231+7021	MLR377AB	R	141.07	0.803	4
2016.994	02471+3533	BU9AB	G	217.19	0.925	4
2016.994	02471+3533	BU9AB	IR742	216.96	0.922	1
2016.994	02471+3533	BU9AB	R	217.31	0.925	4
2016.994	02572+0153	A2413	G	164.92	0.612	1
2016.994	02572+0153	A2413	IR742	174.36	0.495	6
2016.994	02572+0153	A2413	R	165.12	0.619	1
2016.994	02589+2137	BU525	G	274.01	0.551	1
2016.994	02589+2137	BU525	IR742			7
2016.994	02589+2137	BU525	R	274.56	0.536	1

Table 3 continues on next page.

Speckle Interferometry with the OCA Kuhn 22" Telescope

Table 3 (continued). Speckle measurements in 2015 and 2016, using the OCA Kuhn 22-inch telescope, Point Grey BlackFly-U3-23S6M-C CMOS camera, and interference filters. The columns are: observation date, WDS designation, WDS discovery designation, filter (Table 1), position angle observed (degrees), separation observed (arc-seconds), and qualitative figure of merit (Table 2).

Obs Date	WDS	Discovery	Filter	ThetaO	RhoO	Quality
2016.917	03054+2515	STF346AB	G	256.32	0.464	1
2016.917	03054+2515	STF346AB	G	256.09	0.465	1
2016.994	03054+2515	STF346AB	G	255.97	0.450	1
2016.994	03054+2515	STF346AB	IR742	256.22	0.472	1
2016.917	03054+2515	STF346AB	R	257.36	0.462	1
2016.917	03054+2515	STF346AB	R	256.83	0.460	1
2016.994	03054+2515	STF346AB	R	255.97	0.445	1
2015.958	03101+2145	BU1030AB	R	101.93	0.833	1
2015.846	03122+3713	STF360	R	125.47	2.873	4
2015.846	03140+0044	STF367	R	130.71	1.240	6
2015.958	03158+5057	HU544	R	102.76	1.653	1
2015.846	03175+6540	STT52AB	R	56.33	0.484	1
2016.994	03177+3838	STT53AB	G	232.47	0.575	1
2016.994	03177+3838	STT53AB	IR742	232.85	0.568	1
2016.994	03177+3838	STT53AB	R	232.78	0.556	1
2015.846	03184-0056	AC2AB	R	261.84	1.190	1
2015.846	03212+2109	COU259	R	217.82	0.908	1
2015.846	03233+2058	STF381	R	108.45	1.080	1
2016.033	03307-0416	STF408	R	320.21	1.165	1
2015.958	03344+2428	STF412AB	R	351.54	0.766	1
2015.958	03346-3152	B53	R	228.21	1.445	6
2016.994	03350+6002	STF400AB	G	268.41	1.628	1
2016.994	03350+6002	STF400AB	IR742	268.63	1.603	1
2016.033	03350+6002	STF400AB	R	268.49	1.703	1
2016.994	03350+6002	STF400AB	R	268.46	1.612	1
2016.033	03356+3141	BU533AB	R	221.99	1.066	1
2015.958	03362+4220	A1535	R	346.00	0.746	1
2016.033	03362+4220	A1535	R	346.36	0.732	4
2016.033	03377+4807	HLD9AB	R			7
2015.846	03443+3217	BU535	R	20.45	1.052	1
2015.767	03463+2411	BU536AB	R			7
2016.994	03496-0220	YR23	G	294.77	0.355	3
2016.994	03496-0220	YR23	IR742	286.30	0.373	6
2016.994	03496-0220	YR23	R	295.69	0.369	1
2016.994	03503+2535	STT65	G	201.94	0.442	1
2016.994	03503+2535	STT65	IR742	200.86	0.464	1
2016.994	03503+2535	STT65	R	201.85	0.431	1
2016.917	04239+0928	HU304	G	29.54	0.325	2
2016.917	04239+0928	HU304	R	30.57	0.339	2
2016.112	04257-0214	BU 403	G	83.35	0.921	2
2016.112	04275-2427	I 413	G	330.90	0.729	2
2016.112	04279-2130	BU 184	G	247.89	1.917	2
2015.846	04301+1538	STF554	R	15.56	1.465	1
2015.934	04306-2301	HDS580	R			7
2016.112	04308+1609	PAT 11	G			7
2016.112	04316+3739	BU 789	G	323.37	0.919	1
2015.846	04334-1047	HDS592	R			7
2016.112	04349+3908	HU 1082	G	189.86	0.266	6
2016.112	05005+0506	STT 93	G	243.28	1.636	1
2016.112	05043-0602	A 481AB	G	281.77	0.413	3
2016.112	05055+1948	STT 95	G	295.61	0.955	1
2016.112	05059-1355	A 3009	G	274.09	1.226	2
2016.112	05079+0830	STT 98	G	288.94	0.956	1
2016.205	05131+2424	COU 468	G	32.63	0.576	1
2016.205	05135+0158	STT 517AB	G	240.87	0.731	1
2016.205	05140+5126	HU 821	G	171.77	0.826	1
2016.205	05181+0342	A 2639	G	277.24	0.942	1

Table 3 continues on next page.

Speckle Interferometry with the OCA Kuhn 22" Telescope

Table 3 (continued). Speckle measurements in 2015 and 2016, using the OCA Kuhn 22-inch telescope, Point Grey BlackFly-U3-23S6M-C CMOS camera, and interference filters. The columns are: observation date, WDS designation, WDS discovery designation, filter (Table 1), position angle observed (degrees), separation observed (arc-seconds), and qualitative figure of merit (Table 2).

Obs Date	WDS	Discovery	Filter	ThetaO	RhoO	Quality
2016.205	05204-0522	HDS702AaAb	G	234.29	0.642	6
2016.033	05208+3329	COU1231	R	140.96	0.373	3
2016.205	05213+3529	COU 1535	G	99.52	0.359	6
2016.033	05219+3934	COU2037	R	141.98	0.375	3
2016.033	05525+4009	STF802AB	R			7
2015.958	06041+1101	J335	R	270.79	1.274	1
2016.112	06149+2230	BU 1008	G	256.56	1.847	1
2016.112	06221+5922	STF 881AB	G	149.29	0.638	1
2016.112	06256+2227	STT 139	G	257.42	0.791	1
2016.205	06336-1207	HU 43	G	308.30	0.897	1
2016.205	06345-1114	HO 234	G	4.49	0.617	1
2016.112	06364+2717	STT 149	G	279.03	0.752	1
2015.958	06425+6612	MLR318	R	309.13	1.717	1
2016.112	06455+2922	A 122	G	24.48	0.410	3
2016.205	06462+5927	STF 948AB	G	67.31	1.921	1
2016.112	06478+0020	STT 157	G	162.79	0.562	2
2016.205	06487+0737	A 2731AB	G	67.15	1.344	1
2016.205	06555+3010	STF 981	G	299.25	0.925	1
2016.033	06564+0957	HDS960	R	210.19	0.657	6
2015.846	06573+5825	STT159AB	R	235.11	0.710	2
2016.205	07001+4211	COU 2374	G	17.33	0.289	3
2016.033	07003+6720	HDS976	R	188.35	0.382	6
2016.205	07008+2716	BU 1022AB	G	32.10	0.327	3
2016.205	07018-1053	BU 573	G	307.55	0.880	1
2016.205	07028+1305	HO 342	G	88.54	1.201	1
2016.205	08005+0955	A 2954AB	G	337.54	0.647	1
2015.846	08010+2335	STF1171	R	325.80	2.046	4
2016.205	08013-2220	BU 333AB	G	43.15	1.651	2
2016.205	08024+0409	STF 1175	G	287.03	1.419	1
2015.846	08033+2616	STT186	R	76.23	1.077	2
2016.205	08044+1217	BU 581AB	G	214.85	0.353	3
2015.846	08122+1739	STF1196AB	R	19.12	1.120	1
2015.958	08122+1739	STF1196AB	R	18.69	1.153	1
2015.958	08122+1739	STF1196AC	R	61.65	6.345	1
2015.958	08122+1739	HUT1CaCb	R			7
2016.337	09006+4147	KUI 37AB	R	177.07	0.437	5
2016.337	09179+2834	STF 3121AB	R	15.90	0.412	1
2016.337	10279+3642	HU 879	R	226.83	0.543	3
2016.337	10426+0335	A 2768	R	243.68	0.648	1
2016.337	13157+5424	HDS 1858	R			7
2016.337	13166+1948	HDS1862AaAb	R	262.39	0.416	6
2016.337	13189+0341	HDS 1865	R	109.01	1.186	1
2016.337	13202+1534	HDS1870AaAb	R	270.14	0.426	5
2016.337	14426+1929	HU 575AB	R			7
2016.671	15038+4739	STF1909	G	71.27	0.739	1
2016.337	15038+4739	STF1909	R	70.56	0.779	1
2016.671	15038+4739	STF1909	R	71.38	0.743	1
2016.337	15360+3948	STT 298AB	R	185.40	1.194	1
2016.337	15371+2646	HDS2199	R			7
2016.337	15404+2123	HU 579	R			7
2016.337	16309+0159	STF 2055AB	R	42.20	1.373	1
2016.671	16413+3136	STF2084	G	125.51	1.303	1
2016.337	16413+3136	STF 2084	R	126.28	1.252	1
2016.671	16413+3136	STF2084	R	125.06	1.286	1
2016.671	16511+0924	STF2106AB	G	171.54	0.794	1
2016.671	16511+0924	STF2106AB	R	170.54	0.791	1
2016.337	16514+0113	STT 315	R	310.03	0.716	1
2016.337	16518+2840	STF 2107AB	R	104.93	1.436	1

Table 3 continues on next page.

Speckle Interferometry with the OCA Kuhn 22" Telescope

Table 3 (continued). Speckle measurements in 2015 and 2016, using the OCA Kuhn 22-inch telescope, Point Grey BlackFly-U3-23S6M-C CMOS camera, and interference filters. The columns are: observation date, WDS designation, WDS discovery designation, filter (Table 1), position angle observed (degrees), separation observed (arc-seconds), and qualitative figure of merit (Table 2).

Obs Date	WDS	Discovery	Filter	ThetaO	RhoO	Quality
2016.337	17053+5428	STF 2130AB	R	1.58	2.510	1
2016.337	17066+0039	BU 823AB	R	161.86	1.065	4
2016.337	17082-0105	A 1145	R	340.95	0.691	1
2016.671	17130+0745	STT325	G	295.54	0.364	5
2016.671	17130+0745	STT325	R	291.30	0.425	5
2016.337	17141+5608	STT 327	R			7
2016.337	17166-0027	A 2984	R	21.37	0.772	4
2016.761	17304-0104	STF 2173AB	G	142.33	0.646	2
2016.337	17304-0104	STF2173AB	R	143.42	0.661	1
2016.761	17304-0104	STF 2173AB	R	142.60	0.650	1
2016.337	17349+1234	MCY 4	R	235.45	0.537	6
2016.337	17386+5546	STF 2199	R	55.63	1.930	6
2016.671	17400-0038	BU631	G	82.18	0.321	5
2016.671	17400-0038	BU631	R	83.68	0.351	5
2016.671	17471+1742	STF2215	G	250.20	0.451	1
2016.671	17471+1742	STF2215	R	252.57	0.454	1
2016.671	17520+1520	STT338AB	G	162.63	0.846	1
2016.671	17520+1520	STT338AB	R	162.50	0.825	1
2016.671	17571+0004	STF2244	G	100.13	0.695	1
2016.671	17571+0004	STF2244	R	99.85	0.665	1
2016.337	18571+3451	HDS2685	R	199.81	0.550	6
2015.728	19487+1149	STF2583AB	R	105.21	1.487	1
2015.767	19553-0644	STF2597AB	R	99.58	0.720	6
2016.843	20020+2456	STT 395	G	127.04	0.771	1
2016.843	20020+2456	STT 395	IR742	126.75	0.773	1
2016.843	20020+2456	STT 395	R	127.00	0.765	1
2016.671	20320+2548	STF2695	G	259.00	0.359	5
2016.671	20320+2548	STF2695	R	259.47	0.381	5
2016.917	20375+1436	BU151AB	G	185.21	0.318	2
2016.917	20375+1436	BU151AB	G	185.47	0.317	2
2016.917	20375+1436	BU151AB	G	188.75	0.310	2
2016.671	20396+0458	KUI99AB	G	317.87	0.533	6
2016.671	20396+0458	KUI99AB	R	321.35	0.583	6
2016.761	20474+3629	STT 413AB	G	1.37	0.931	1
2016.761	20474+3629	STT 413AB	R	1.47	0.937	1
2016.761	20519+0544	A 613	G	319.94	0.670	4
2016.761	20519+0544	A 613	R	318.15	0.671	1
2016.761	20524+2008	HO 144	G	350.01	0.435	1
2016.761	20524+2008	HO 144	R	352.04	0.448	1
2016.843	21026+2141	BU 69AB	G	10.65	0.283	6
2016.843	21026+2141	BU 69AB	IR742			7
2016.843	21026+2141	BU 69AB	R	4.98	0.382	5
2016.761	21135+0713	BU 270AB	G	346.54	0.490	6
2016.761	21135+0713	BU 270AB	R	351.67	0.455	1
2016.671	21137+6424	H1-48	G	244.15	0.684	1
2016.671	21137+6424	H1-48	R	244.02	0.689	1
2016.671	21148+3803	AGC13	G	197.54	0.944	1
2016.671	21148+3803	AGC13	R	197.21	0.938	1
2016.671	21186+1134	BU163AB	G	257.16	0.903	1
2016.671	21186+1134	BU163AB	R	257.72	0.905	1
2015.767	21352+2124	BU74	R	337.73	0.979	1
2016.671	21395-0003	BU1212AB	G	302.30	0.314	1
2015.767	21395-0003	BU1212AB	R	301.17	0.336	3
2016.671	21395-0003	BU1212AB	R	298.07	0.371	5
2016.671	21426+4103	BU688AB	G	197.56	0.373	1
2016.671	21426+4103	BU688AB	R	195.43	0.406	1

Table 3 concludes on next page.

Speckle Interferometry with the OCA Kuhn 22" Telescope

Table 3 (conclusion). Speckle measurements in 2015 and 2016, using the OCA Kuhn 22-inch telescope, Point Grey BlackFly-U3-23S6M-C CMOS camera, and interference filters. The columns are: observation date, WDS designation, WDS discovery designation, filter (Table 1), position angle observed (degrees), separation observed (arc-seconds), and qualitative figure of merit (Table 2).

Obs Date	WDS	Discovery	Filter	ThetaO	RhoO	Quality
2016.671	21555+1053	BU75AB	G	25.80	1.052	1
2016.671	21555+1053	BU75AB	R	25.38	1.066	1
2015.767	22029+4439	BU694AB	R	5.95	1.018	1
2015.767	22044+1339	STF2854	R	83.71	1.601	1
2016.843	22057+3521	PRU 2	G			7
2016.843	22057+3521	PRU 2	IR742	4.05	0.453	6
2015.767	22057+3521	PRU2	R			7
2015.958	22057+3521	PRU 2	R			7
2016.843	22057+3521	PRU 2	R			7
2015.934	22365+5826	PRU3	R	5.14	0.365	5
2016.843	22388+4419	HO 295AB	G	336.10	0.318	1
2016.843	22388+4419	HO 295AB	IR742	336.12	0.360	5
2016.843	22388+4419	HO 295AB	R	336.29	0.325	3
2015.846	22400+0113	A2099	R	164.92	0.840	4
2016.843	22402+3732	HO 188	G	230.64	0.361	1
2016.843	22402+3732	HO 188	IR742			7
2016.843	22402+3732	HO 188	R	228.39	0.351	3
2015.846	22409+1433	HO296AB	R	51.59	0.465	1
2015.934	22437+4725	HDS3224	R			7
2015.846	22478-0414	STF2944AB	R	304.65	1.866	1
2015.958	22514+2623	HO482AB	R	13.36	0.518	2
2015.846	22514+6142	STF2950AB	R	275.20	1.182	1
2016.843	22520+5743	A 632	G	110.12	0.359	2
2016.843	22520+5743	A 632	IR742	108.31	0.378	5
2016.843	22520+5743	A 632	R	109.31	0.379	1
2016.843	22537+4445	BU 382AB	G	244.92	0.676	1
2016.843	22537+4445	BU 382AB	IR742	245.98	0.638	1
2016.843	22537+4445	BU 382AB	R	244.80	0.685	1
2015.934	23029+0738	HDS3282	R			7
2016.843	23072+6050	BU 180AB	G	133.02	0.544	4
2016.843	23072+6050	BU 180AB	IR742			7
2016.843	23072+6050	BU 180AB	R	134.06	0.541	4
2016.994	23176+1818	HU400	G	70.26	0.344	6
2016.994	23176+1818	HU400	IR742			7
2016.994	23176+1818	HU400	R	67.52	0.349	6
2016.761	23241+5732	STT 495	G	120.43	0.404	1
2016.761	23241+5732	STT 495	R	120.14	0.407	1
2016.843	23375+4426	STT 500AB	G	13.83	0.439	1
2016.843	23375+4426	STT 500AB	IR742	12.83	0.462	1
2016.843	23375+4426	STT 500AB	R	12.71	0.423	1
2015.728	23413+3234	BU858AB	R			7
2015.728	23420+2018	STT503AB	R	134.50	1.233	1
2015.846	23440+2922	AGC14	R	283.95	0.857	4
2016.843	23516+4205	STT 510AB	G	300.81	0.609	1
2016.843	23516+4205	STT 510AB	IR742	295.27	0.619	2
2016.843	23516+4205	STT 510AB	R	300.29	0.619	1
2016.994	23595+3343	STF3050AB	G	340.17	2.469	1
2016.994	23595+3343	STF3050AB	R	340.22	2.452	1
2016.994	23595+3343	STF3050AB	IR742	340.24	2.439	1
2016.994	23595+3343	STF3050AD?	G	38.67	4.280	4
2016.994	23595+3343	STF3050AD?	R	38.27	4.292	4
2016.994	23595+3343	STF3050AD?	IR742	37.85	4.315	4

the primary peak may indicate that the peaks above and below are artifacts of atmospheric dispersion, due to the zenith angle greater than 30 degrees. Additional observations are needed.

The Table 3 observation of **02231+7021 MLR377AB** is uncertain at best (figure of merit 6). The STB auto-correlogram in Figure 7 had the weakest secondary peaks of all the stars observed. Although these measured peaks were the brightest in the field, there are numerous other possible candidates which are likely just noise and not faint stars. In the orbit plot, even though the current observation continues the trend diverging from the premature orbit, it seems too far from the other points. The proper motions of the two components are the same, although they are small.

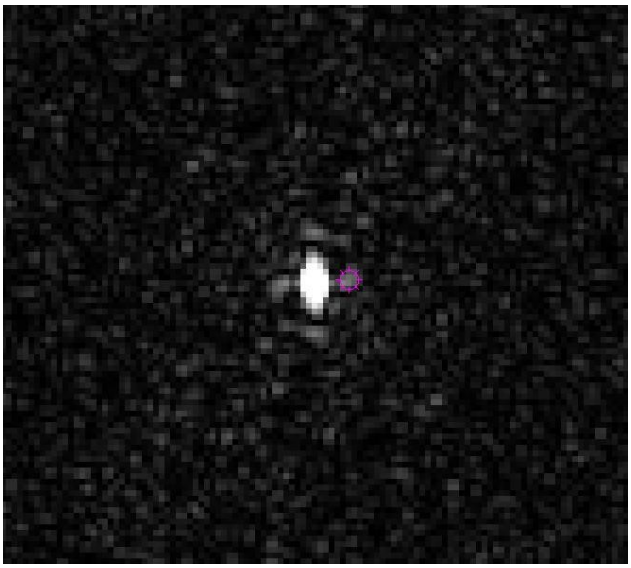

Figure 6. The STB auto-correlogram of TDS2201. The secondary peaks are barely above the background noise.

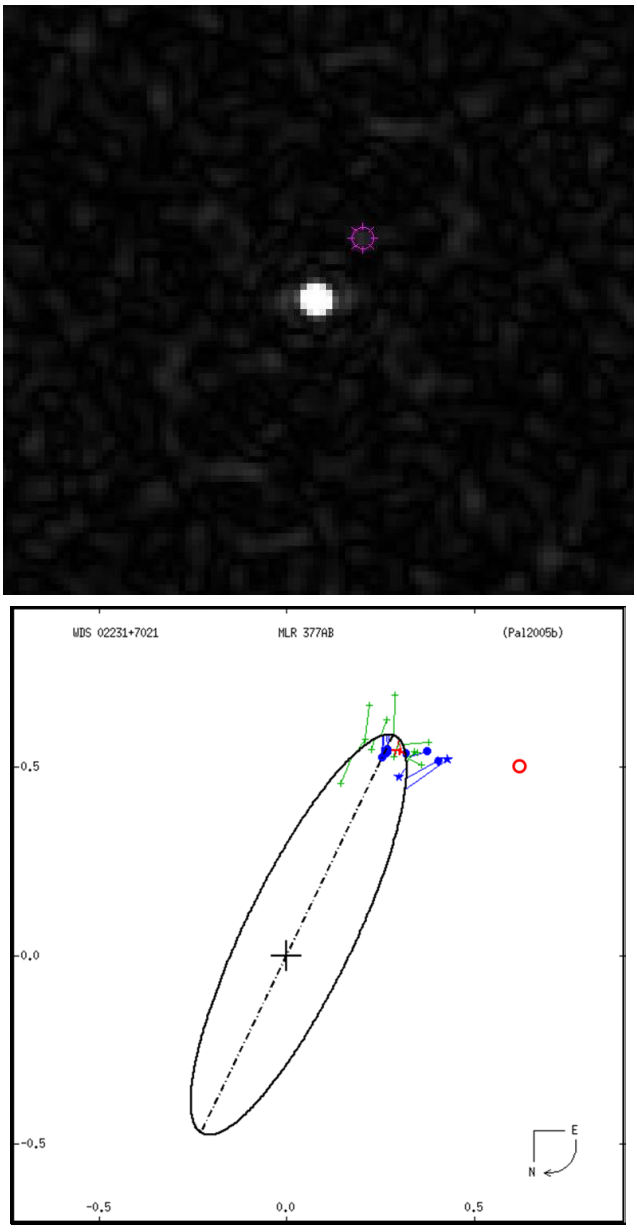

Figure 7. Top: The STB auto-correlogram of MLR377AB. Bottom: The position of the current uncertain measure (red circle) generally continues the diverging trend of earlier speckle points.

Speckle Interferometry with the OCA Kuhn 22" Telescope

The binary **03175+6540 STT52AB** has a Grade 4 orbital period of 350 years, but most of the recent speckle points are diverging from that orbit, shown in Figure 8, including the observation of Table 3. The speckle points show a roughly linear trend of increasing separation, so the period is likely much longer, but the earliest micrometer points (green +), and the same proper motion of both components, still demand that this is a binary.

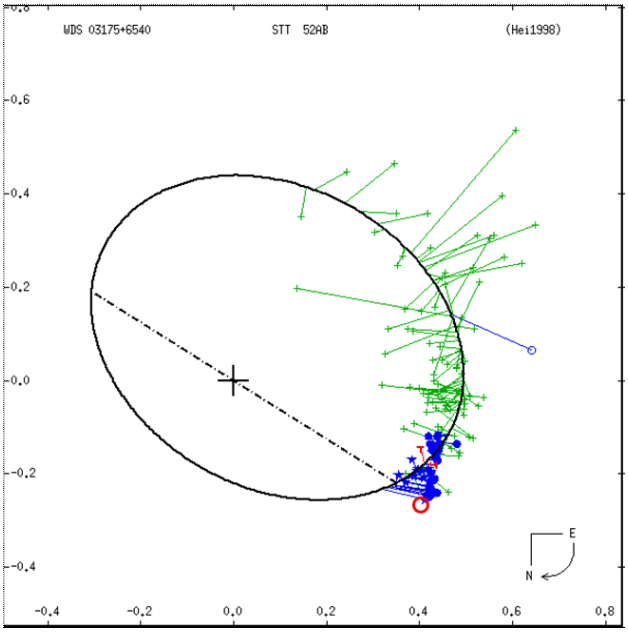

Figure 8. The orbit of binary star STT52AB, from the Washington Double Star 6th Orbit Catalog. The point from Table 3 is indicated by the red circle.

05208+3329 COU1231 was discovered visually by Paul Couteau in 1975 (Couteau, 1976). There are very few observations in the WDS archives, all of which are plotted in Figure 9. There were no observations from 1975 to 2000, then four speckle observations from 2000 to 2010. No other observations were available in the WDS. The current observation of Table 3 was in early 2016.

In the top-left part of Figure 9, all the points are plotted as given in WDS. However, the distribution of points seems peculiar - the discovery point (+) of Couteau, a very experienced observer, seems out of place, and the general trend shows little movement in the first 25 years, but fast closure in the most recent 6 years. For these reasons, all the speckle points from 2000 to 2016 were plotted with 180 degrees added to the PA, as shown in the top-right part of Figure 9. This distribution, which assumed that the observation of Couteau had the only correct PA quadrant because it was obtained visually, looks reasonable, suggesting a high-inclination orbit with a period on the order of only five or six decades.

To help clarify the situation, a request was made to Dave Rowe, who is developing a new bi-spectral tool for his Speckle Tool Box program, to do bi-spectral

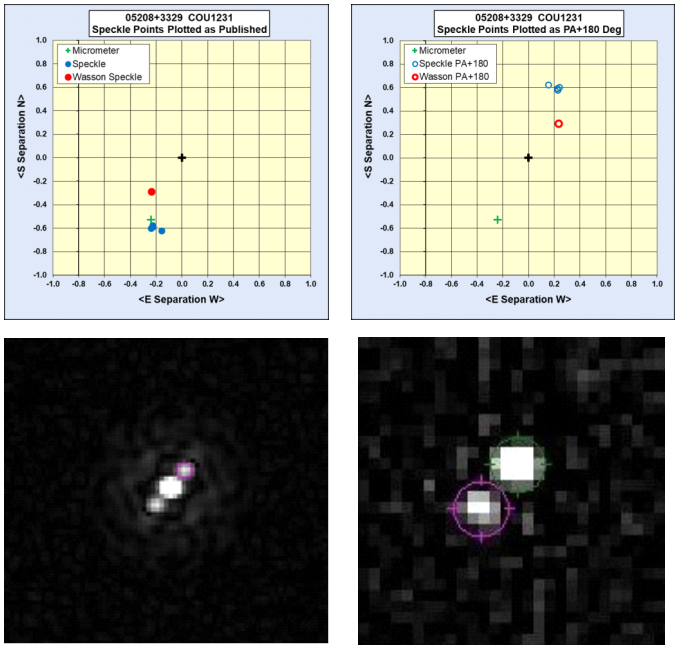

Figure 9. Upper Left: All observations of COU1231 from the WDS are plotted, together with the new point from Table 3, indicated by the solid red circle. (Note: north up, east left, as on the sky). Upper Right: Speckle points are plotted with 180 degrees added to the PA values from WDS and Table 3. Lower Left: The current auto-correlogram. Lower Right: The bispectrum image of COU1231, courtesy of Dave Rowe, clearly shows that the PA of the companion is in the second (southeast) quadrant.

analysis of my speckle images. The result (Rowe, 2017), shown at lower-right of Figure 9, confirms that the speckle PA observations are properly located in the second quadrant, as given in WDS.

06149+2230 BU1008 is a very bright semiregular variable (V=3.3-3.9) red giant (Eta Gem, M3.5I-II), 2.6 magnitudes brighter than its companion. All speckle points are diverging from the grade 5 preliminary orbit, including the Hipparcos/Tycho measures. The Table 3 measure continues that trend, as seen in Figure 10. Therefore, the period is likely longer than the 474-year orbit. However, since the motion so far seems roughly linear, the pair may also be only optical.

06256+2227 STT139: This pair was observed in February 2016 with the G filter, but the measured separation was larger than the WDS last observation and much larger than the orbit ephemerides. Figure 11 shows the WDS orbital plot, with the current point added. Only one other speckle point is available since the Hipparcos/Tycho observations. However, since emerging from periastron, the trend is clearly diverging into a wider orbit, just as the early micrometer points indicated before periastron. Perhaps the observations merit an updated orbit solution.

The class 2 orbit of **08044+1217 BU581AB**, with a period of 45 years, is now approaching a full revolution

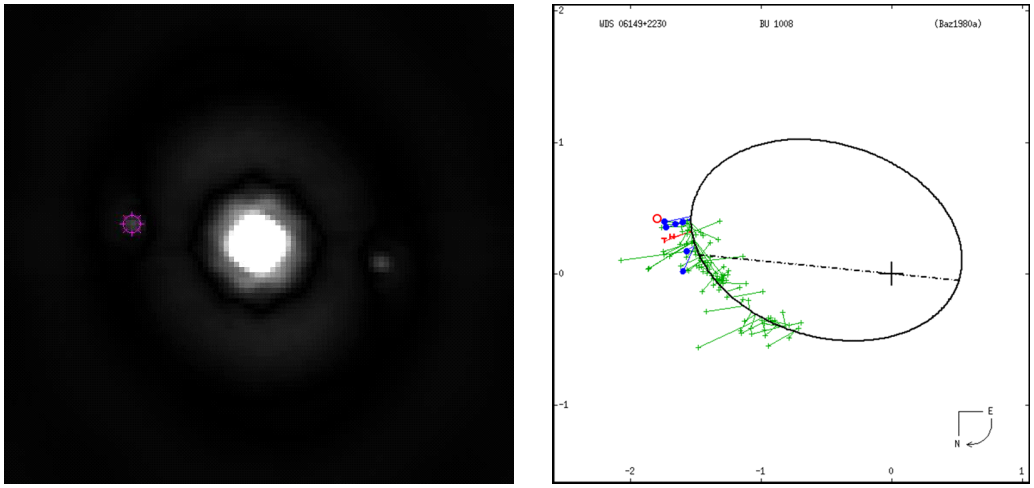

Figure 10. Left: The STB auto-correlogram of BU1008. Right: The position of the current measure (red circle) continues the generally diverging trend of the other speckle points.

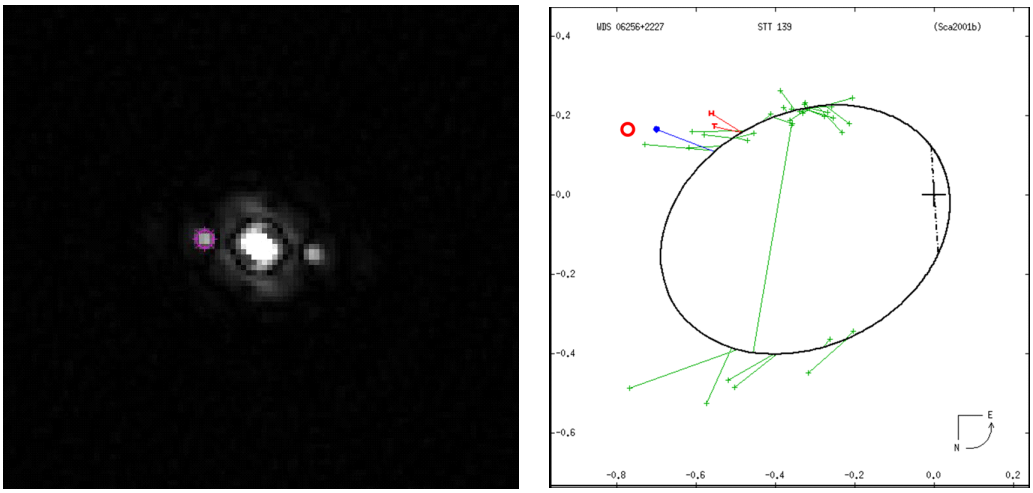

Figure 11. Left: STB auto-correlogram of STT139. Right: The current measure (red circle) supports a clear trend toward a larger orbit, based on the other speckle point, Hipparcos, Tycho, and early micrometer points.

Speckle Interferometry with the OCA Kuhn 22" Telescope

of speckle measurements. The Table 3 measure, shown in Figure 12, is a little inside the orbit solution, but helps fill in the gap since the last WDS plotted speckle point in 2006. Two other recent speckle points from 2008 and 2010, are available in the WDS observation database, but not yet shown on its orbit plot. These were added to Figure 12 as blue circles. Additionally, an observation taken with the same OCA 22-inch telescope early in 2017, but with a different camera, is slightly outside the orbit line (black circle), and will be published later. This pair deserves more frequent speckle observations.

22365+5826 PRU3 is the very luminous variable *supergiant* star W Cephei, which pulsates from orange to red in color and has the strange spectral type K0Iapev. It has very small proper motion (-3, -2) and the huge distance, based on Hipparcos measurements, is over 100,000 light years. Although it is a spectroscopic binary, the visible companion, only 1.3 magnitudes fainter, is unlikely to be gravitationally bound, but is almost certainly a much nearer star. Therefore, the relative motion should be linear. Only two prior measures have been made, one by Hipparcos (1991) and one by speckle (1997). There were also two unresolved speckle observations on 2-meter telescopes (closer than 0.05") within 2 years of the successful speckle observation. It is possible that these may have failed because the primary variability increased the delta magnitude. The current observation in Table 3 is uncertain, but the PA which is more consistent with linear motion - moving farther apart in roughly the same direction – was selected for Table 3. If this trend is true, a few further observations should confirm it.

The binary **22409+1433 HO296AB** was observed in November 2015, chosen as a bright double with a well-known orbit, but challengingly close for the 22-inch. HO296AB, whose orbit it shown in Figure 13, is one of the few binaries which has a Grade 1 "definitive" orbit solution, meaning it has numerous accurate measurements over at least one full orbit. The period is 20.83 years, so the orbit has been fully covered by speckle measurements, begun in 1979 by Dr.

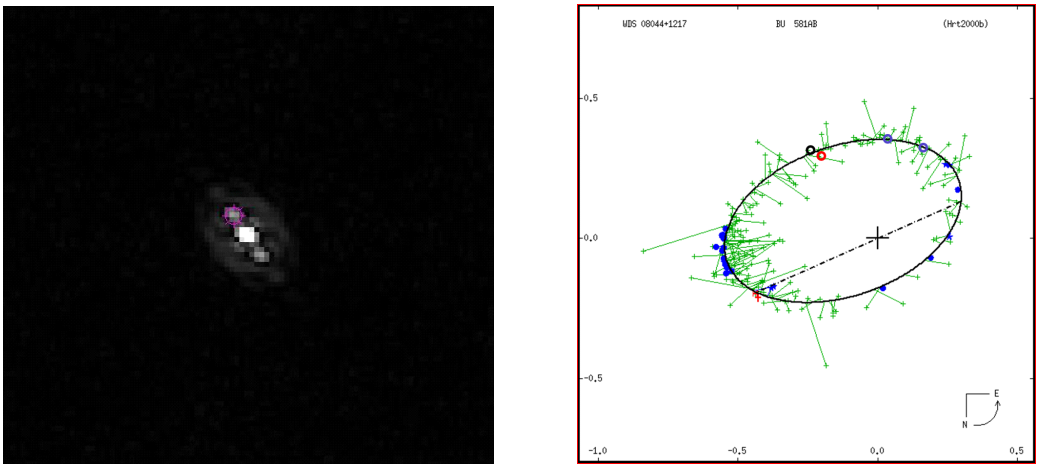

Figure 12. Left: STB autocorrelogram of BU581AB. Right: The measure of Table 3 (red circle) helps fill in the gap in speckle observations. Two additional speckle points which are in the WDS archive but not yet plotted, are shown as blue circles, while the black circle is a 2017 observation by the author.

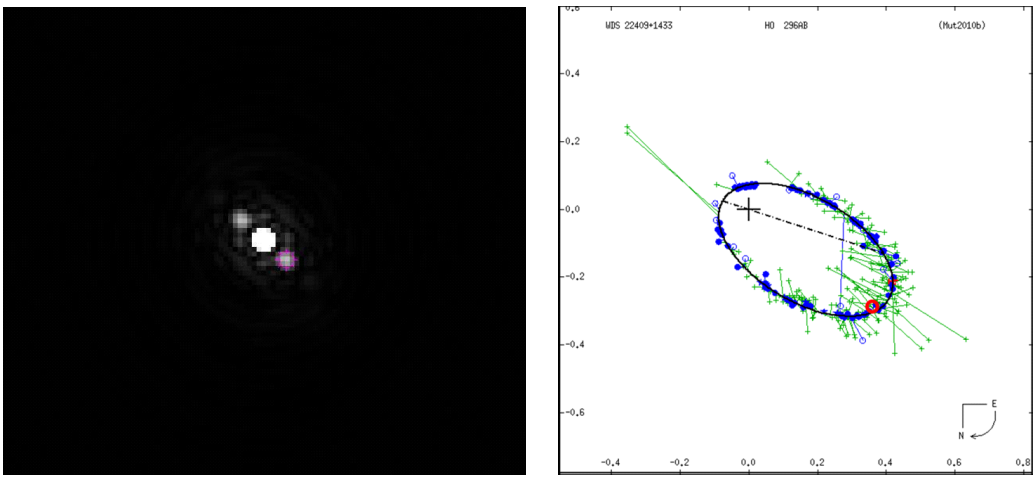

Figure 13. Left: STB autocorrelogram of HO296AB. Right: The point in Table 3 is the red circle at lower right, in reasonably good agreement with the Class 1 orbit.

Speckle Interferometry with the OCA Kuhn 22" Telescope

Harold McAlister on the Kitt Peak 4-meter Mayall telescope. Almost all the other speckle observations were also made by professional astronomers with telescopes including the Kitt Peak 2.1m, WIYN 3.5m, Mt. Wilson 2.5m (100"), and the Discovery Channel 4.3m. In addition, near periastron, where the separation is less than 0.1 arc-second, measurements have been made with the Russian 6m telescope (speckle in 1983) and with the Palomar Test Bed Interferometer (2003 through 2008). Not until after I reduced the data and compared my measurement with the historical data of others, did I realize what distinguished company I had inadvertently joined.

The auto-correlograms of **23595+3343 STF3050** are shown in Figure 14, in all three filters of Table 1. The top row shows the AB components. However, the bottom row has been over-exposed to show an additional faint star at about 4.3" separation and 38 degrees PA, as given in Table 3. Of course, the PA of this object may be actually 180 degrees from Table 3.

This object cannot be the faint C component (magnitude 12.8), because WDS lists it about 80 arc-sec distant from A; therefore, this could be a new "D" component. However, this system has been very well observed in the past, with more than 600 published observations in the WDS archives. Therefore, it is extremely unlikely that this star, which is probably brighter than the C component, has been overlooked by all previous observers.

Indeed, a plot of the three measurements of Table 3, Figure 15, shows small but roughly linear motion, consistent with the order in which the exposure sequences were made: G, R, IR742. All sequences were 1000 exposures of 0.030 sec each. The mid-time of the R sequence was 50.4 sec after the mid-time of the G sequence, while the IR742 sequence was 45.2 sec after the R sequence. Therefore, the "new" component was moving about 0.044 arc-sec per minute toward the north-west (or south-east).

The faint object shows up in the double star auto-correlations, with and without using the reference star for deconvolution, and it does not appear in the reference autocorrelation alone; therefore, it is not an artifact from a faint companion near the reference star, as may sometimes occur. Although it was about 33 degrees north of the ecliptic, which is near zero declination at RA~24 hours, this object may be an interloping asteroid.

However, a cursory search found no asteroid with a well-known orbit near the double star at the time. Two

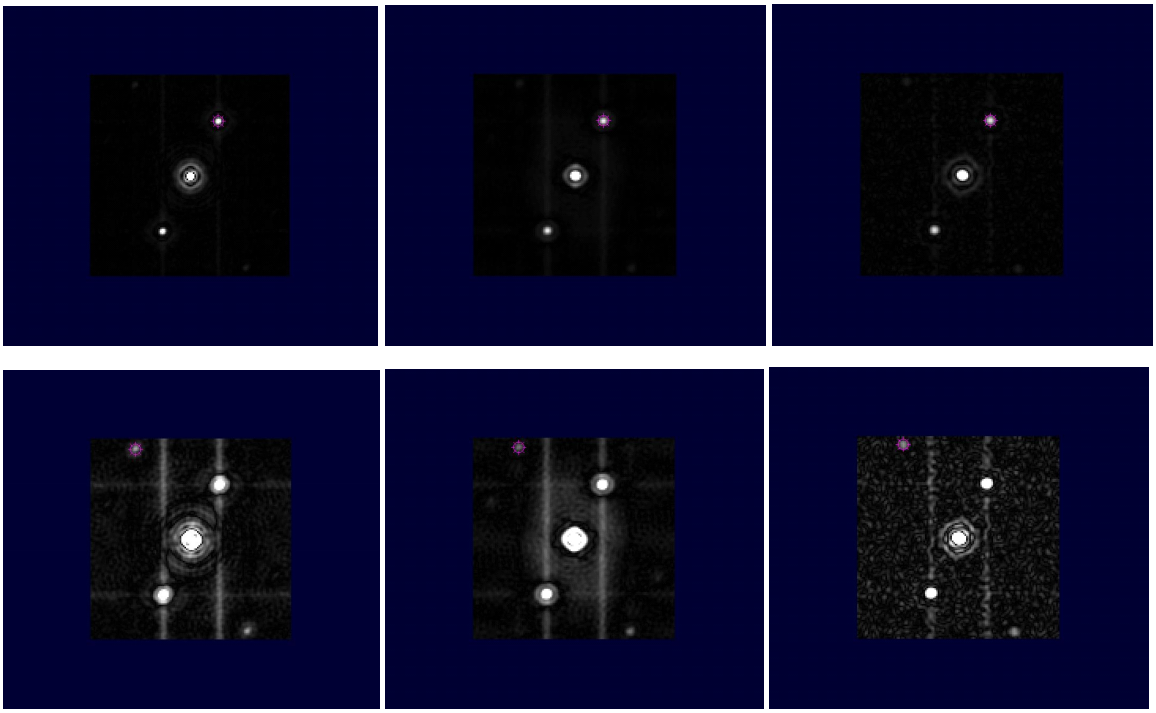

Figure 14. Top Row: STB auto-correlograms of STF3050AB in all three filters of Table 1: G (left), R (middle) and IR742-pass (right). Bottom Row: The same auto-correlograms, shown over-exposed to reveal an additional faint star. The vertical and horizontal streaks are artifacts probably caused by CMOS line pattern ("read") noise related to the bright B component. The STB interference filter can suppress line pattern noise related to the primary star, because it is always at the center of the field after FFT processing.

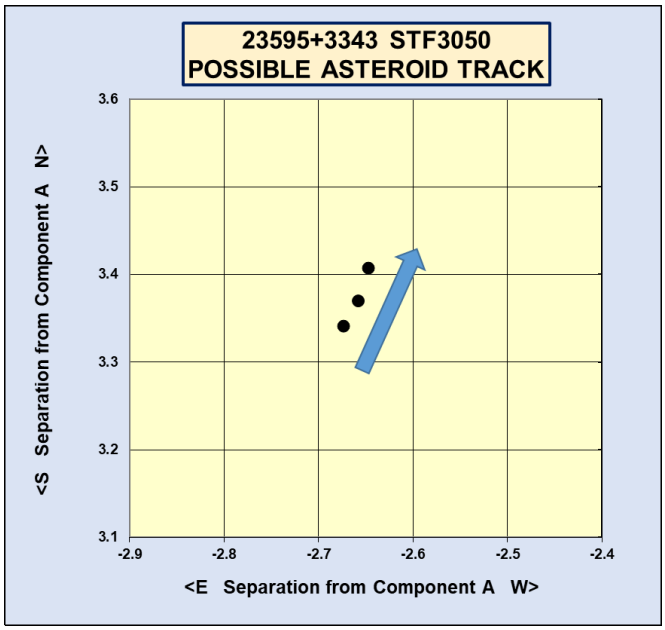

Figure 15. The Table 3 offsets (arc-seconds) of the "new" component of STF3050, relative to the A component, for the G, R and IR742 filter sequences. The arrow indicates the order of the three sets of exposures, and therefore, the direction of travel. Because of the speckle 180-degree ambiguity, the actual motion may be in the opposite direction.

other remote possibilities may be a small, near-earth asteroid, or an old geosynchronous satellite, out of fuel and drifting far from the original equatorial region. Unfortunately, this object remains a mystery.

Acknowledgements

The author is very grateful to OCA President Barbara Toy for her dedication and expertise in instructing new Star Members, and her custodianship of the Kuhn 22-inch Telescope, and to members of the Orange County Astronomers for support and maintenance of the Anza site facilities. He also thanks Dave Rowe, Russ Genet, and Bob Buchheim for their inspiration, correspondence, instruction, and assistance along the speckle journey.

This research has made use of the Washington Double Star Catalog, the 6th Orbit Catalog, and the Observation Catalog, all maintained at the U.S. Naval Observatory, and the author particularly thanks Brian Mason for providing all previous observation data for requested stars.

References

Bryant, Tom, 2015. http://mainsequence.org/html/wds/getListOfDoubles/listWithOrbits.html

Buchheim, R. K., 2017. *Journal of Double Star Observations*, **13**, 233-236, April, 2017.

Couteau, P., 1976. *A&AS*, **24**, 495.

Edelmann, Torsten, 2015. FireCapture2.4. http://firecapture.wonderplanets.de

Harshaw, Richard and Rowe, David and Genet, Russell, 2017. "The Speckle Toolbox: A Powerful Data Reduction Tool for CCD Astrometry." *Journal of Double Star Observations*, **13**, 52-67, January 1, 2017.

Losse, Florent, 2015. "REDUC 4.72." http://www.astrosurf.com/hfosaf.

Rowe, David A. and Genet, Russell M., 2015. "User's Guide to PS3 Speckle Interferometry Reduction Program." *Journal of Double Star Observations*, **11**, 266-276.

Rowe, David A., 2016. Yahoo Group speckleinterferometry@yahoo.com.

Rowe, David A., 2017. Private communication.

Sordiglioni, Gianluca, 2016. http://stelledoppie.goaction.it/index2.php?section=1.

Wasson, Rick, 2014. "Measuring Double Stars with a Dobsonian Telescope by the Video Drift Method." *Journal of Double Star Observations*, **10**, 324-341.